Title: Phenology and diversity in Zambia

Authors: Godlee J. L.[1], Ryan C. M.[1], Siampale A.[2], Dexter K. G.[1,3]

[1]School of GeoSciences, University of Edinburgh, Edinburgh, United Kingdom

[2]Forestry Department Headquarters - Ministry of Lands and Natural Resources, Cairo Road, Lusaka, Zambia

[3]Royal Botanic Garden Edinburgh, Edinburgh, EH3 5LR, United Kingdom

Corresponding author:

John L. Godlee

johngodlee@gmail.com

School of GeoSciences, University of Edinburgh, Edinburgh, United Kingdom

Acknowledgements

Author constribution statement

JLG conceived the study, conducted the analysis, and wrote the first draft of the manuscript. AS coordinated plot data collection in Zambia, and initial data management. All authors contributed to manuscript revisions.

Data accessibility statement

The data used in this study are held by the Zambian Integrated Land Use Assessment Project (ILUA-II), and were cleaned by the SEOSAW project (Socio-ecological Observatory for Southern African Woodlands). The data are not publicly available at the time of submission due to privacy concerns surrounding plot location, but can be requested from the corresponding author. An anonymised version will be made available in a data repository following review.

Main Text

Title: Phenology and diversity in Zambia

Abstract

1 Introduction

The seasonal timing and duration of foliage production (land-surface phenology) is a key mediator of land-atmosphere exchanges. Foliage forms the primary interface between plants, the atmosphere and sunlight (Gu et al., 2003; Penuelas, Rutishauser, and Filella, 2009), thus land-surface phenology plays an important role in regulating global carbon, water and nitrogen cycles (). Carbon-cycling models routinely incorporate land-surface phenological processes, most commonly through remotely-sensed data products (**Bloom2016**), but our understanding of the ecological mechanisms which determine these phenological processes remains sparse. This limits our ability to predict how land-surface phenology will respond to climate change, and how these repsonses will vary among species and vegetation types ().

At regional scales, land-surface phenology can be predicted using only climatic factors, namely precipitation, diurnal temperature, and light environment (Adole, Jadunandan Dash, and Peter M. Atkinson, 2018b), but significant local variation exists within biomes in the timing of leaf production which cannot be attributed solely to abiotic environment (). It has been repeatedly suggested that the diversity and functional composition of plant species plays a role in determining how ecosystems respond to abiotic phenological cues (Adole, Jadunandan Dash, and Peter M. Atkinson, 2018a; Jeganathan, J. Dash, and P. M. Atkinson, 2014; Fuller, 1999), owing to differences in life history strategy among species and demographic groups, but current implementations of biotic variation in carbon cycling models is limited to coarse plant functional types, which are unable to represent the wide variation in phenological patterns observed within biomes (Scheiter, Langan, and Higgins, 2013; Pavlick et al., 2013).

Across the dry tropics, seasonal oscillations in water availability produce strong cycles of foliage production (), with knock-on effects for ecosystem function and structure (). The phenomenon of pre-rain green-up seen in some tree species within the dry tropics serves as a striking example of adaptation to seasonal variation in water availability (**See in and also Ryan2017**). Conservative species, i.e. slower growing, with robust leaves and denser wood, may initiate leaf production (green-up) before the rainy season has commenced. More acquisitive species and juveniles however, tend to green-up during the rainy season creating a dense leaf-flush during the mid-season peak of growth and dropping their leaves earlier as the wet season ends (). Both strategies have associated costs and benefits which allow species exhibiting a range of phenological syndromes along this spectrum to co-exist. While conservative species gain a competitive advantage from having fully emerged leaves when the rainy season starts, they must also invest heavily in deep root architecture to access dry season groundwater reserves in order to produce foliage during the dry season. Similarly, while acquisitive species minimise the risk of hydraulic failure and mortality by only producing leaves when conditions are amenable, they forfeit growing season length (). It has been suggested that variation in phenological strategy among tree species is one mechanism by which increased species diversity increases resilience to drought and maximises productivity in water-limited woodland ecosystems (). By providing functional redundancy within the ecosystem, leaf production can be maintained under a wider range of conditions, therefore maximising long-term productivity.

In addition to determining productivity and biomass, variation in leaf phenology also affects broader ecosystem function. Woodlands with a longer tree growth period support a greater diversity and abundance of wildlife, particularly bird species, but also browsing mammals and invertebrates (Cole et al., 2015; Araujo et al., 2017; Morellato et al., 2016; Ogutu, Piepho, and Dublin, 2013). As climate change increases the frequency and severity of drought in water-limited woodlands, it is feared that this will result in severe negative consequences for biodiversity (Bale et al., 2002). The periods of green-up and senescence which bookend the growing season are key times for invertebrate reproduction (), soil biotic activity () and herbivore browsing activity (). Pre-rain green-up provides a valuable source of moisture and nutrients before the rainy season, and can moderate the understorey microclimate, increasing humidity, reducing UV exposure, and moderating diurnal oscillations in temperature, reducing ecophysiological stress which can lead to mortality during the dry season. Earlier pre-rain green-up provides a buffer to stressful dry season climatic conditions (). Additionally, a slower rate of green-up caused by tree species greening at different times, i.e. reduced synchronicity, provides an extended period of bud-burst, maintaining the important food source of nutrient rich young leaves for longer (). Thus, understanding the determinants of seasonal patterns of tree leaf production in dry deciduous woodlands can provide valuable information on spatial variation in vulnerability to climate change, and help to model their contribution to land surface carbon cycle models under climate change.

In this study we investigated how tree species diversity and composition influence three key measurable aspects of the tree phenological cycle of dry tropical woodlands: (1) the rates of greening and senescence at the start and end of the seasonal growth phase, (2) the overall length of the growth period, and (3) the lag time between green-up/senescence and the start/end of the rainy season. It is hypothesised that: (H_1) due to variation among species in minimum viable water availability for growth, plots with greater tree species richness will exhibit slower rates of greening and senescence as different species green-up and senesce at different times. We hypothesise that: (H_2) in plots with greater species richness the start of the growing season will occur earlier with respect to the onset of rain due to an increased likelihood of containing a species which can green-up early. We hypothesise that: (H_3) plots with greater species richness will exhibit a longer growth period and greater cumulative green-ness over the course of the growth period, due to a higher resilience to variation in water availability. Finally, we hypothesise that: (H_4) irrespective of species diversity, variation in tree species composition and vegetation type will cause variation in the phenological metrics outlined above.

2 Materials and methods

2.1 Plot data

We used plot-level data on tree species diversity and composition across 705 sites from the Zambian Integrated Land Use Assessment Phase II (ILUA-II), conducted in 2014 (Mukosha and Siampale, 2009; Pelletier et al., 2018). Each site consisted of four 20x50 m (0.1 ha) plots positioned in a square around a central point, with a distance of 500 m between each plot (Figure 2). The original census contained 993 sites, which was filtered in order to define study bounds and to ensure data quality. Only sites with $\geq$50 stems ha^{-1} $\geq$10 cm DBH (Diameter at Breast Height) were included in the analysis, to ensure all sites represented woodlands rather than 'grassy savanna', which is considered a separate biome with different species composition and ecosystem processes governing phenology (Parr et al., 2014). Sites dominated by non-native tree species ($\geq$50% of individuals), e.g. *Pinus* spp. and *Eucalyptus* spp. were excluded, as these species may exhibit non-seasonal patterns of foliage production (). Of the trees recorded, % were only identified to genus, and % could not be identified.

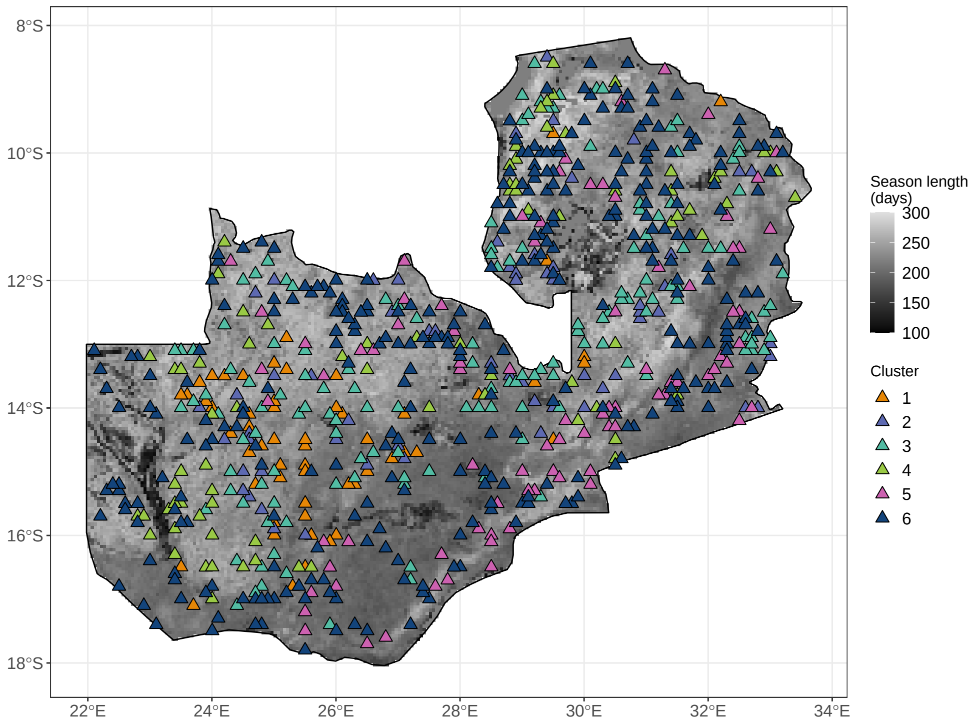

Figure 1: Distribution of study sites within Zambia as triangles, each consisting of four plots. Sites are oloured according to vegetation compositional cluster as identifed by Ward's clustering algorithm on euclidean distance of plots in the first two axes of NSCA ordination space. Zambia is shaded according to growing season length as estimated by the MODIS VIPPHEN-EVI2 product, at 0.05° spatial resolution (Didan and Barreto, 2016).

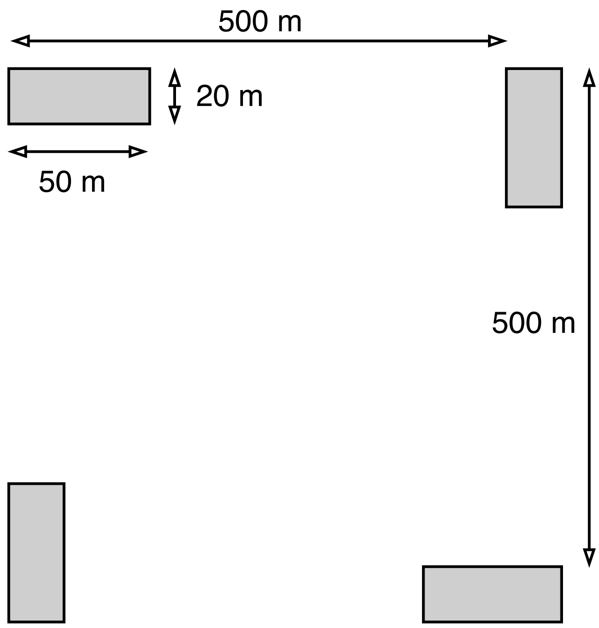

Figure 2: Schematic diagram of plot layout within a site. Each 20x50 m (0.1 ha) plot is shaded grey. The site centre is denoted by a circle. Note that the plot dimensions are not to scale.

Within each plot, the species of all trees with at least one stem ≥10 cm DBH were recorded. Plot data was aggregated to the site level for analyses to avoid pseudo-replication caused by the more spatially coarse phenology data. Tree species composition varied little among the four plots within a site, and were treated as representative of the woodland in the local area. Using the Bray-Curtis dissimilarity index of species abundance data, we calculated that the mean pairwise compositional distance between plots within a site was lower than the mean compositional distance across all pairs of plots in 88.4% of cases.

2.2 Land-surface phenology data

To quantify phenology at each site, we used the MODIS MOD13Q1 satellite data product at 250 m resolution (Didan, 2015). The MOD13Q1 product provides an Enhanced Vegetation Index (EVI) time series at 16 day intervals. EVI is widely used as a measure of vegetation growth, as an improvement to NDVI (Normalised Differential Vegetation Index), which tends to saturate at higher values. Annual cumulative EVI is well-correlated with gross primary productivity and so can act as a suitable proxy (). We used all scenes from January 2010 to December 2020 with less than 20% cloud cover covering the study area. All sites were determined to have a single annual growth season according to the MODIS VIPPHEN product (), which assigns pixels (0.05°, 5.55 km at equator) up to three growth seasons per year. We stacked yearly data between 2010 and 2020 and fit a General Additive Model (GAM) to produce an average EVI curve. We estimated the start and end of the growing season using first derivatives of the GAM. Start of the growing season was identified as the first day where the model slope exceeds half of the maximum positive model slope for a continuous period of 20 or more days, using only backwards looking data, following White et al. (2009). Similarly, we defined the end of the growing season as the final day of the latest 20 period where the GAM slope meets or exceeds half of the maximum negative slope. We estimated the length of the growing season as the number of days between the start and end of the growing season. We estimated the green-up rate as the slope of a linear model across EVI values between the start of the growing season and the point at which the slope of reduces below half of the maximum positive slope. Similarly the senescence rate was estimated as the slope of a linear model between the latest point where the slope of decrease fell below half of the maximum negative slope and the end of the growing season Figure 3. We validated our calculations of cumulative EVI, mean annual EVI, growing season length, season start date, season end date, green-up rate and senescence rate with calculations made by the MODIS VIPPHEN product with linear models comparing the two datasets across our study sites (Figure S1, Table S1). We chose not to use the MODIS VIPPHEN product directly due to its more coarse spatial resolution (0.05°, 5.55 km at equator). Sites where our calculation of a phenological metric was drastically different to the MODIS VIPPHEN estimate were excluded, under the assumption that our algorithm had failed to capture the true value or some site specific factor precluded precise estimation. This removed 8 sites.

Precipitation data was gathered using the "GPM IMERG Final Precipitation L3 1 day V06" dataset, which has a pixel size of 0.1°(11.1 km at the equator) (Huffman et al., 2015), between 2010 and 2020. Daily total precipitation was separated into two periods: precipitation during the growing season (growing season precipitation), and precipitation in the 90 day period before the onset of the growing season (dry season precipitation). Rainy season limits were defined as for the EVI data, using the first derivative of a GAM to create a curve for each site using stacked yearly precipitation data, from which we estimated the half-max positive and negative slope to identify where the GAM model exceeded these slope thresholds for a consistent period of 20 days or more. Mean diurnal temperature range (Diurnal δT) was calculated as the mean of monthly temperature range from the WorldClim database, using the BioClim variables, with a pixel size of 30 arc seconds (926 m at the equator) (Fick and Hijmans, 2017). averaged across all years of available data (1970-2000). We calculated the lag between the onset of the growing season and the onset of the rainy season as the difference between these two dates as calculated above. We performed a similar calculation to estimate the lag between the end of the growing season and the end of the rainy season.

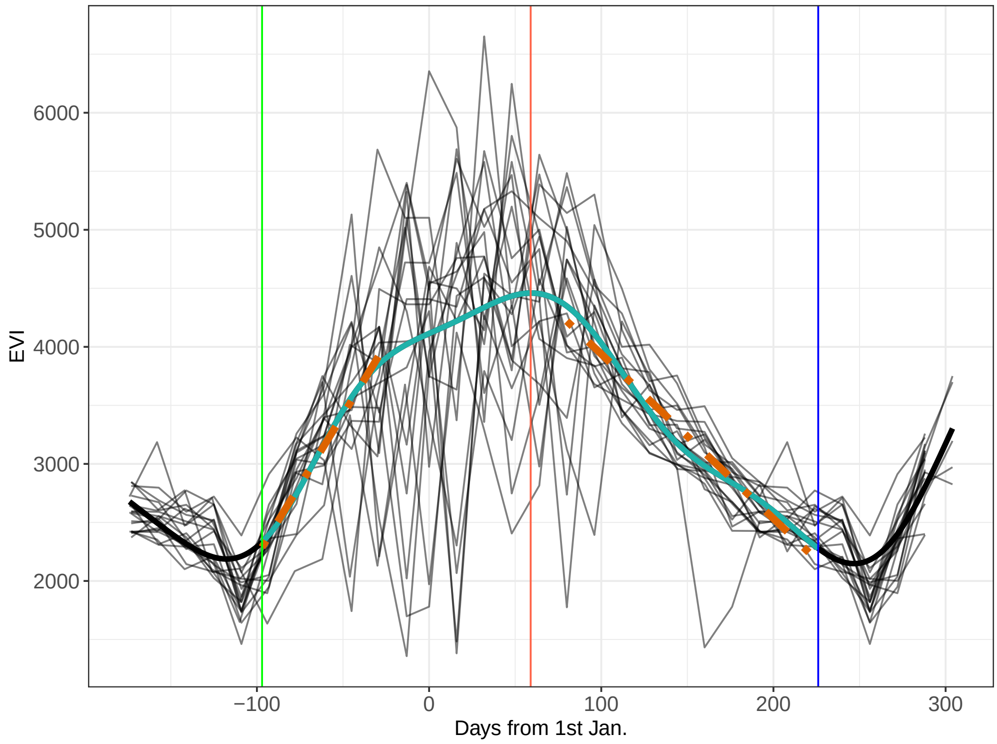

Figure 3: Example EVI time series, demonstrating the metrics derived from it. Thin black lines show the raw EVI time series, with one line for each annual growth season. The thick black line shows the GAM fit. The thin blue lines show the minima which bound the growing season. The red line shows the maximum EVI value reached within the growing season. The shaded cyan area of the GAM fit shows the growing season, as defined by the first derivative of the GAM curve. The two orange dashed lines are linear regressions predicting the green-up rate and senescence rate at the start and end of the growing season, respectively. Note that while the raw EVI time series fluctuate greatly around the middle of the growing season, mostly due to cloud cover, the GAM fit effectively smooths this variation to estimate the average EVI during the mid-season period.

2.3 Data analysis

To measure variation in tree species composition we a used combination of Non-symmetric Correspondence Analysis (NSCA) and agglomerative hirerarchical clustering on species basal area weighted data (Kreft and Jetz, 2010; Fayolle et al., 2014). NSCA was performed using the `ade4` R package (Dray and Dufour, 2007). Scree plot analysis demonstrated that 2 axes was optimal to describe our data. These axes accounted for 17.9% of the variance in species composition according to eigenvalue decay. To guard against sensitivity to rare individuals, which can preclude meaningful cluster delineation across such a large species compositional range, we restricted the NSCA to species with five or more records, and to sites with more than five species (). We used Ward's algorithm to define clusters (Murtagh and Pierre Legendre, 2014), based on the euclidean distance of sites in

NSCA ordination space. We determined the optimal number of clusters by maximising the mean silhouette width among clusters (Rousseeuw, 1987) Figure S3. Vegetation type clusters were used later as interaction terms in linear models. We described the vegetation types represented by each of the clusters using a Dufrene-Legendre indicator species analysis (Dufrêne and P. Legendre, 1997).

To describe the species diversity of each site, we calculated the Shannon-Wiener index (H') from species basal area rather than individual abundance, as a measure of species richness effectively weighted by a species' contribution to canopy occupancy (). H' was then transformed to the first order numbers-equivalent (^1D) of H', calculated as $e^{H'}$ (). We use ^1D as the primary measure of species richness in our statistical models and is subsequently referred to as such. Additionally, we calculated a separate measure of abundance evenness, using the Shannon Equitability index ($E_{H'}$) (Smith and Wilson, 1996). $E_{H'}$ was calculated as the ratio of basal area Shannon-Wiener diversity index to the natural log of total basal area per site.

2.3.1 Statistical modelling

We specified multivariate linear models to assess the role of tree species diversity on each of the chosen phenological metrics. We defined a maximal model structure including richness, abundance evenness, the interaction of richness and vegetation type, and climatic variables shown by previous studies to strongly influence phenology. The quality of the maximal model was compared to models with different subsets of independent variables using the model log likelihood, AIC (Akaike Information Criteria), BIC (Bayesian Information Criteria), and adjusted R^2 values for each model. For each phenological metric, the best model according to the model quality statistics is reported in the results. Where two similar models were within 2 AIC points of each other, the model with fewer terms was chosen as the best model, to maximise model parsimony. All models were fitted using Maximum Likelihood (ML) to allow comparison of models (). The best model was subsequently re-fitted using Restricted Maximum Likelihood for model effect estimation (REML). Independent variables in each model were transformed to achieve normality where necessary and standardised to Z-scores prior to modelling to allow comparison of slope coefficients within a given model.

To describe variation within and among vegetation types in their land-surface phenology we conducted a principal component analysis of the six phenological metrics we derived from the MOD13Q1 product. We also conducted a simple MANOVA using the phenological metrics as response variables, followed by post-hoc Tukey's tests between each pairwise combination of vegetation types per phenological metric, to test whether vegetation types differed significantly in their land-surface phenology.

We used the `ggeffects` package to estimate the marginal means of the interaction effect of species diversity and vegetation type, to investigate vegetation type specific effects on each phenological metric (Lüdecke, 2018). Estimated marginal means entails generating model predictions across values of a focal variable, in this case species diversity, while holding non-focal variables constant. All statistical analyses were conducted in R version 4.0.2 (R Core Team, 2020).

3 Results

Model selection showed that richness and evenness are important determinants of each of the chosen phenological metrics, across vegetation types. The effect of richness featured and was significant in all best models except for senescence laf and senescence rate. Evenness was a significant effect in models for cumulative EVI, season length and senescence lag only Figure 4.

3 vegetation type clusters were identified during hierarchical clustering. Cluster 3, which contains the most sites (487), consists of small stature Zambesian woodlands, as referenced by Dinerstein et al. (2017) and Chidumayo (2001), and is not dominated by a particular large canopy tree species. It is possible that these woodlands represent highly disturbed woodlands where large trees may have been removed by humans. Abundance evenness is high across sites in Cluster 3. Cluster 2 is dominated heavily by *Brachystegia boehmii*, while Cluster 1 is dominated by *Julbernardia paniculata*, both large canopy-forming trees. These two clusters likely represent variation among miombo woodland types in dominant canopy tree species. Both Clusters 1 and 2 have a similar composition of non-dominant smaller shrubby species, such as *Pseudolachnostylis maprouneifolia* (Table 1).

As expected (H_3), richness and wet season precipitation both had positive significant effects on cumulative EVI and season length. In contrast, abundance evenness, the other aspect of tree species diversity in our models, had a significant negative effect on both cumulative EVI and season length (Figure 4).

Species richness caused a significant increase in the lag time between date of green-up and date of rainy season onset (H_2). This effect was comparable to the effects of pre-season precipitation and diurnal temperature range, which also caused an increase in green-up lag. In contrast, senescence lag was poorly defined by our models, suggesting that some unmeasured factor remains the key driver of this phenological metric. The effects of diurnal δT and abundance evenness had wide confidence interval. The best model explained only 1% of the variance in senescence lag, though was still better quality than a climate-only model.

All best models including tree species diversity variables were of better quality than models which included only climatic variables Table 2. The phenological metrics best predicted were green-up lag and cumulative EVI, where models explained 26% and 34% of the variance in these variables, respectively. Senescence rate and senescence lag were the least well predicted phenological metrics, with the best model explaining 3% and 2% of their variance, respectively.

While species richness had a significant negative effect on green-up rate, as predicted by H_1, the best model, which also included pre green-up precipitation and diurnal temperature range, only explained 10% of the variance in this metric.

The slope of the relationship between species richness and phenological metrics varied among vegetation types, in all models except the model for green-up lag, vegetation types with both positive and negative signs were observed Figure 5. Across all models however, none of the vegetation types were significantly different, according to post-hoc Tukeys's tests on marginal effects (Table S8). Clusters were largely similar in their density distribution of the six phenological metrics Figure 7, and a MANOVA followed by post-hoc Tukey's tests showed no significant differences between any pairwise combination of vegetation types for any phenological metric. The most striking differences are the presence of some sites in Cluster 5 with particularly high green-up rates. The hierarchical clustering analysis demonstrated that there was little spatial structure to the vegetation clusters identified. The key emergent trends were that Clusters 2 and 5 were absent from the southwest of the country (Figure 1) possibly due to the low levels of precipitation in this region, which could preclude many miombo tree species. Additionally Cluster 1 was predominantly restricted to the central western part of the country.

Cluster	N sites	Richness	MAP	Diurnal δT	Species	Indicator value
					Julbernardia paniculata	0.712
1	91	13(6)	966(139.7)	14(1.3)	*Psuedolachnostylis maprouneifolia*	0.222
					Pericopsis angolensis	0.209
					Brachystegia boehmii	0.764
2	127	16(6)	1054(162.5)	13(1.5)	*Psuedolachnostylis maprouneifolia*	0.234
					Uapaca kirkiana	0.227
					Pterocarpus angolensis	0.333
3	487	15(7)	1037(195.9)	14(1.6)	*Brachystegia spiciformis*	0.318
					Diplorhynchus condylocarpon	0.298

Table 1: Climatic information and Dufrene-Legendre indicator species analysis for the vegetation type clusters identified by the PAM algorithm, based on basal area weighted species abundances. The three species per cluster with the highest indicator values are shown along with other key statistics for each cluster. MAP (Mean Annual Precipitation) and Diurnal δT are reported as the mean and 1 standard deviation in parentheses. Species richness is reported as the median and the interquartile range in parentheses.

Response	δAIC	δBIC	R^2_{adj}	δlogLik
Cumulative EVI	12.5	3.3	0.26	-8.23
Season length	10.7	6.1	0.10	-6.37
Green-up rate	3.5	-5.7	0.11	-3.77
Senescence rate	19.9	-7.7	0.05	-15.95
Green-up lag	58.8	49.6	0.28	-31.42
Senescence lag	0.1	0.1	0.05	-0.05

Table 2: Model fit statistics for each phenological metric.

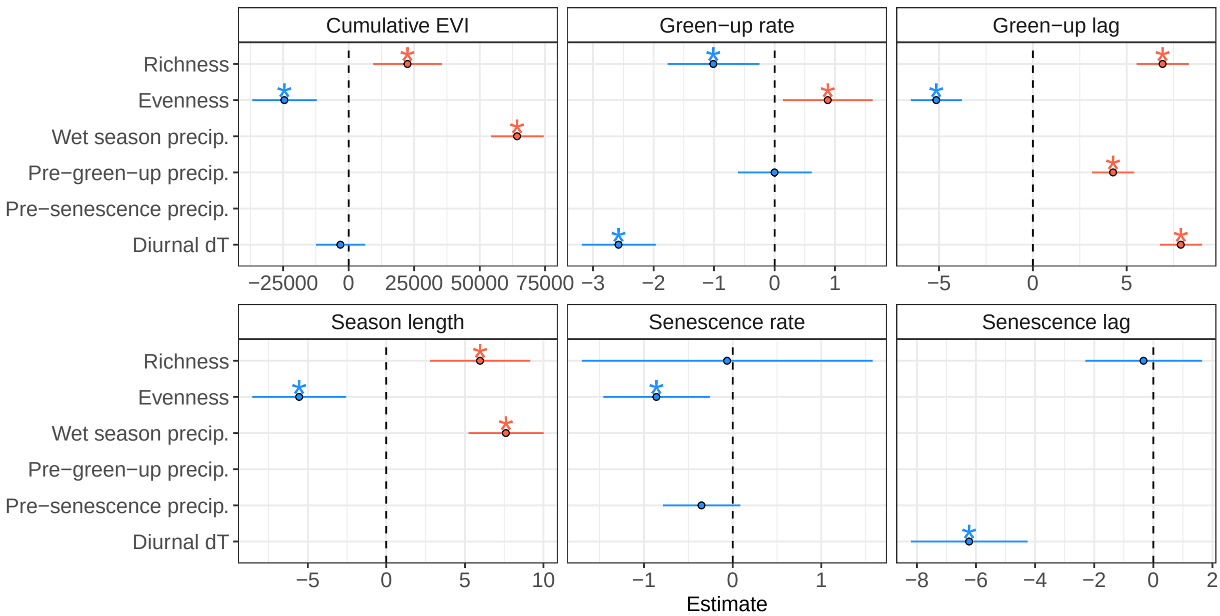

Figure 4: Standardized slope coefficients for each best model of a phenological metric. Slope estimates are ± 1 standard error. Slope estimates where the interval (standard error) does not overlap zero are considered to be significant effects.

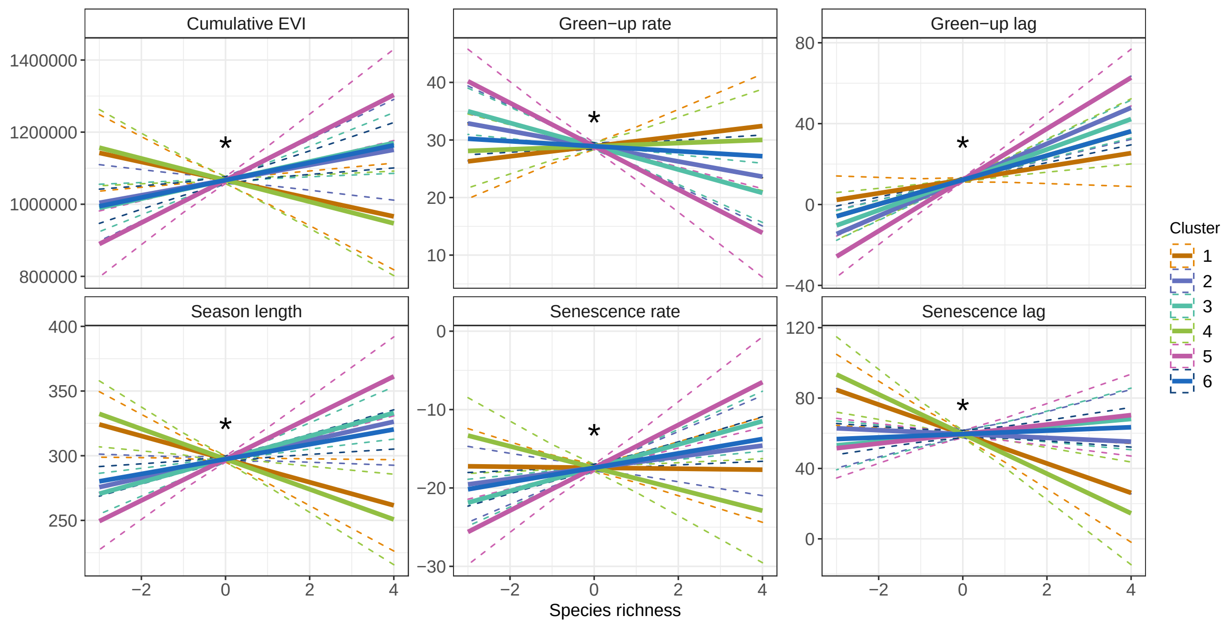

Figure 5: Marginal effects of tree species richness on each of the phenological metrics, for each vegetation type, using the best model including the interaction of species richness and vegetation cluster, for each phenological metric.

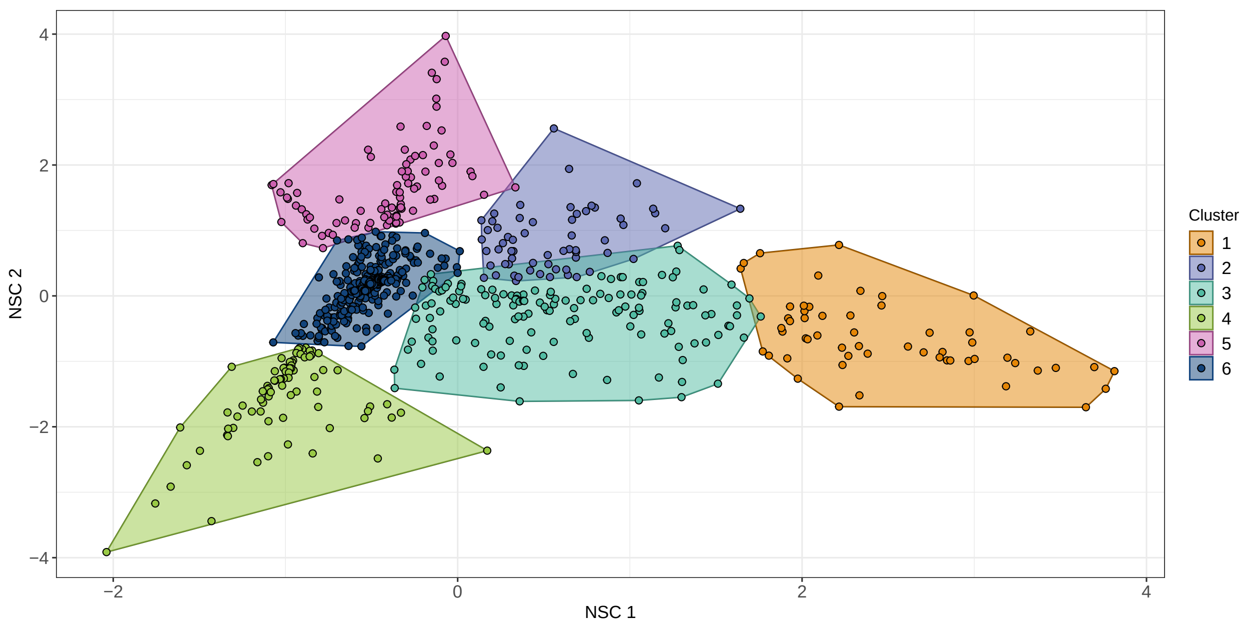

Figure 6: Plot scores of the (A) first and second, and (B) third and fourth axes of the Non-Symmetric Correspondence Analysis of tree species composition. Points are coloured according to clusters defined by Ward's algorithm on euclidean distances of the NSCA ordination axes, along with a convex hull encompassing 95% of the points in each cluster.

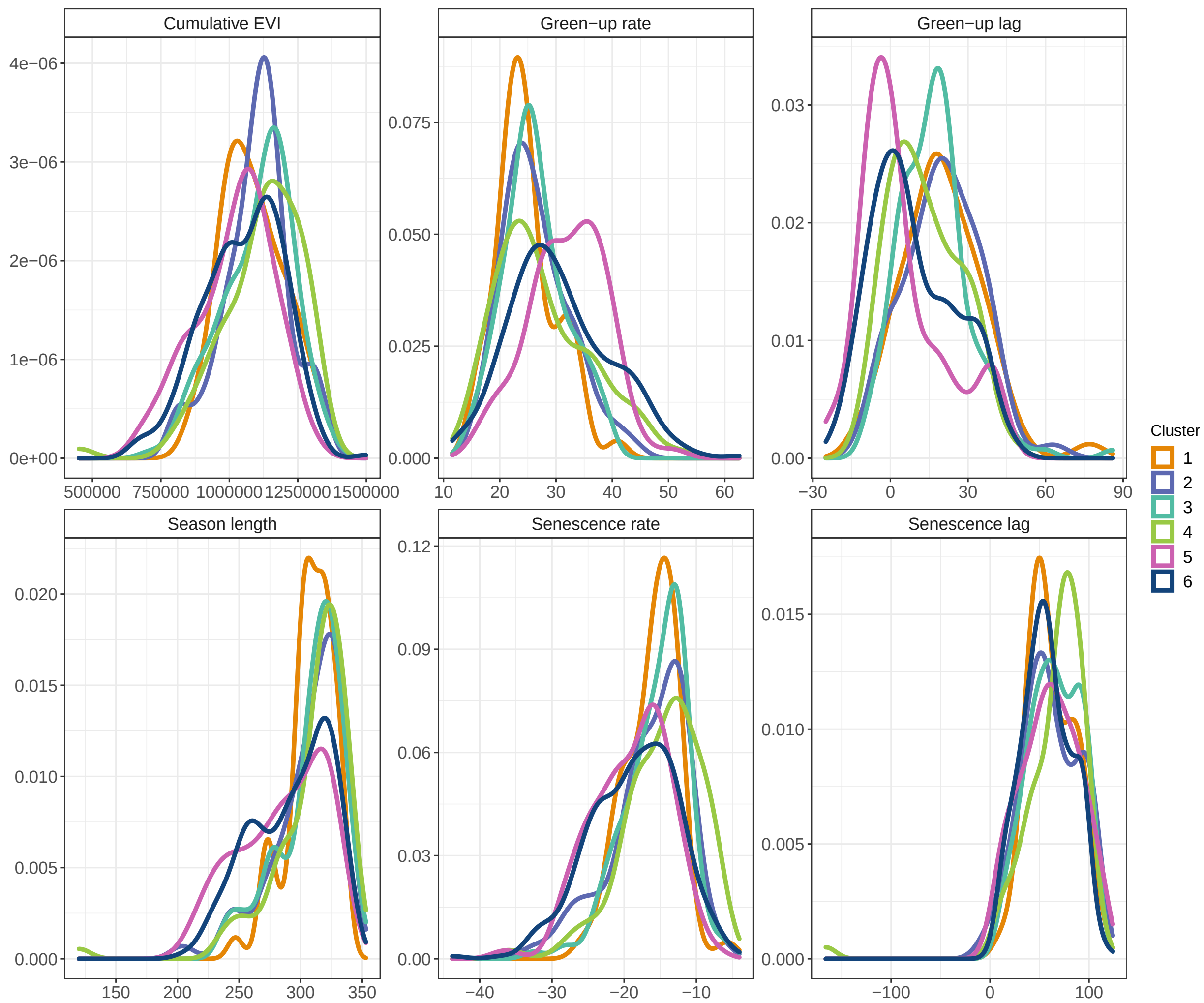

Figure 7: Density distribution of the six phenological metrics used in the study, grouped by vegetation type cluster. For a pairwise comparison of phenological metrics and their correlations, see Figure S2 and **??**.

4 Discussion

In this study we have demonstrated a clear and measurable effect of tree species richness across various aspects of land-surface phenology in Zambian deciduous savannas. We showed that tree species richness led to an increase in cumulative EVI and season length. Additionally, species richness led to a slower rate of greening and caused the onset of greening to occur earlier with respect to the start of the rainy season. Our study lends support for a positive biodiversity - ecosystem function relationship in our chosen study area, operating through its influence on phenology. Our results exemplify the key role of tree species biodiversity in driving key ecosystem processes, which affect ecosystem structure, the wildlife provisioning role, and the gross primary productivity of ecosystems.

Our finding that species richness strongly affects patterns of land-surface phenology in deciduous savannas has important consequences for two pertinent fields of ecological research. Firstly, it should prompt conservation scientists to take advantage of remotely sensed land-surface phenology data to improve estimates of tree species diversity. The technology behind remote-sensing of tree species diversity is maturing fast, providing a means to rapidly and accurately assess the conservation priority of biodiversity hotspots, and to identify regions suffering biodiversity loss. Secondly, it can provide earth surface system modellers with a means to better understand how future changes in species diversity and composition will affect land-surface phenology and therefore the carbon cycle. Incorporating predictions of biotic change into carbon models has been slow, owing to large uncertainties in the effects of diversity on Gross Primary Productivity (GPP). Our study provides a link by demonstrating a strong positive relationship between species richness and EVI, which itself drives GPP.

Patterns of senescence were poorly predicted by species richenss and evenness in our models. Cho, Ramoelo, and Dziba (2017) found that tree cover, measured by MODIS LAI data, had a significant effect on senescence rates in savannas in South Africa, which have similar climatic conditions to the sites in our study. In sparse savannas, while the onset of the growing season is often driven by tree photosynthetic activity, which may precede the onset of precipitation, the end of the growing season is conversely driven by grasses (). Grass activity is much more reactive to short-term changes in soil moisture than tree activity, and may oscillate within the senescence period. This may explain the lack of a strong precipitation signal for senescence lag and senescence rate. Other studies both global and within southern African savannas have largely ignored patterns of senescence, instead focussing patterns of green-up (**Gallinat2015**). Most commonly, these studies simply correlate the decline of rainfall with senescence, but the lack of precipitation as a term in our best model suggests that other unmeasured factors are at play. Alternatively, **Zani2020** suggests that in resource limited environments, senescence times may largely be set by the preceding photosynthetic activity and sink-limitations on growth. For example, limited nutrient supply may prohibit photosynthesis late in the season if the preceding photosynthetic activity has depleted that supply. **Reich1992** suggested that there may be direct constraints on leaf life-span, especially in disturbance and drought-prone environments such as those studied here, which would lead to senescence rate being set largely by the time since bud-burst. In our study however, we found that there was variation in season length between plots, indicating that there are additional factors at play.

While leaf senescence is not as important for the survival of browsing herbivores as green-up, the timing of senescence with respect to temperature and precipitation has important consequences for the savanna understorey microclimate. The longer leaf material remains in the canopy after the end of the rainy season, the greater the microclimatic buffer for herbaceous understorey plants and animals, which require water and protection from high levels of insolation and dry air which can prevail rapidly after the end of the rainy season (). Our study merely exemplifies that more work needs to be done to properly characterise the drivers of senescence in this biome.

While species richness is a common measure of biodiversity, abundance evenness constitutes a second key axis (Wilsey et al., 2005; Hillebrand, Bennett, and Cadotte, 2008). While traditionally species richness and evenness were assumed to be highly positively correlated, recent work has demonstrated that in many systems, richness and evenness may be nearly orthogonal (). In this study, we found contrasting effects of richness and evenness on both cumulative EVI and season length. Evenness caused a decrease in these phenological metrics, which we did not expect. It is possible that the negative effect of abundance evenness occurred because an increase in evenness is associated with a reduction in the canopy cover of a few highly dominant large canopy tree species (e.g. *Brachystegia boehmii* and *Julbernardia paniculata*), as part of the transition from woody savanna to thicket vegetation, or following a major disturbance event. Large canopy tree species have access to ground water for a longer part of the year, due to their deep root systems and conservative growth patterns. A future study may choose to explore the differential effects of species diversity in different size classes and in different physiognomic groups defined by functional form, e.g. shrub, canopy tree, coppicing tree.

Our coverage of very short season lengths in Zambia, as estimated by the VIPPHEN product, was restricted, with notable absences of plot data in the northeast of the country around 30.5°E, 11.5°S, and 23.0°E, 15.0°S. Upon further inspection of true colour satellite imagery, these regions are largely seasonally water-logged floodplain and swampland, and were likely ignored by the ILUA-II assessment for this reason. This also explains their divergent phenological patterns as observed in the MODIS EVI data.

It is important to note that the remotely sensed EVI measurements used here aren't specific only to trees, they represent the landscape as a singe unit. Nevertheless, seasonal patterns of tree leaf phenology in southern African deciduous woodlands, particularly the pre-rainy season green-up phenomenon, is driven almost exclusively by trees, while grasses tend to follow patterns of precipitation more closely (). Grasses contribute to gross primary productivity, and it was therefore in our interests to include their response in our analysis as we seek to demonstrate how tree species richness can affect cycles of carbon exchange. Additionally, the micro-climatic effects of tree leaf canopy coverage and hydraulic lift through tree deep root systems will benefit the productivity of grasses as well as understorey tree individuals.

It is possible that not all tree individuals in our dataset exhibited a completely deciduous growth pattern. Some highly conservative species in this region remain evergreen throughout the dry season. **MORE**.

5 Conclusion

Here we explored the role of tree species diversity on land surface phenology across Zambia. We showed that species richness clearly affects rate of green-up, the lag time between rainy season onset and growth, and the length of the growing season. Our results have a range of consequences for earth system mdoellers and conservation managers, and lend further support to an already well established corpus of the positive effect of species diversity on ecosystem function.

References

Adole, Tracy, Jadunandan Dash, and Peter M. Atkinson (2018a). "Characterising the land surface phenology of Africa using 500 m MODIS EVI". In: *Applied Geography* 90, pp. 187–199. DOI: 10.1016/j.apgeog.2017.12.006. URL: https://doi.org/10.1016%2Fj.apgeog.2017.12.006.

– (2018b). "Large-scale prerain vegetation green-up across Africa". In: *Global Change Biology* 24.9, pp. 4054–4068. DOI: 10.1111/gcb.14310.

Araujo, Helder F. P. de et al. (2017). "Passerine phenology in the largest tropical dry forest of South America: effects of climate and resource availability". In: *Emu - Austral Ornithology* 117.1, pp. 78–91. DOI: 10.1080/01584197.2016.1265430.

Bale, Jeffery S. et al. (2002). "Herbivory in global climate change research: direct effects of rising temperature on insect herbivores". In: *Global Change Biology* 8.1, pp. 1–16. DOI: 10.1046/j.1365-2486.2002.00451.x.

Chidumayo, E. N. (2001). "Climate and Phenology of Savanna Vegetation in Southern Africa". In: *Journal of Vegetation Science* 12.3, p. 347. DOI: 10.2307/3236848.

Cho, Moses A., Abel Ramoelo, and Luthando Dziba (2017). "Response of Land Surface Phenology to Variation in Tree Cover during Green-Up and Senescence Periods in the Semi-Arid Savanna of Southern Africa". In: *Remote Sensing* 9.7, p. 689. DOI: 10.3390/rs9070689.

Cole, Ella F. et al. (2015). "Predicting bird phenology from space: satellite-derived vegetation green-up signal uncovers spatial variation in phenological synchrony between birds and their environment". In: *Ecology and Evolution* 5.21, pp. 5057–5074. DOI: 10.1002/ece3.1745.

Didan, L. (2015). *MOD13Q1 MODIS/Terra Vegetation Indices 16-Day L3 Global 250m SIN Grid V006 [Data set]*. NASA EOSDIS Land Processes DAAC. DOI: 10.5067/MODIS/MOD13Q1.006. (Visited on 08/05/2020).

Didan, L. and A. Barreto (2016). *NASA MEaSUREs Vegetation Index and Phenology (VIP) Phenology EVI2 Yearly Global 0.05Deg CMG [Data set]*. NASA EOSDIS Land Processes DAAC. DOI: 10.5067/MEaSUREs/VIP/VIPPHEN_EVI2.004. (Visited on 08/05/2020).

Dinerstein, Eric et al. (2017). "An Ecoregion-Based Approach to Protecting Half the Terrestrial Realm". In: *BioScience* 67.6, pp. 534–545. DOI: 10.1093/biosci/bix014.

Dray, Stéphane and Anne–Béatrice Dufour (2007). "The ade4 Package: Implementing the Duality Diagram for Ecologists". In: *Journal of Statistical Software* 22.4, pp. 1–20. DOI: 10.18637/jss.v022.i04.

Dufrêne, M. and P. Legendre (1997). "Species assemblage and indicator species: the need for a flexible asymmetrical approach". In: *Ecological Monographs* 67, pp. 345–366. DOI: 10.1890/0012-9615(1997)067[0345:SAAIST]2.0.CO;2.

Fayolle, Adeline et al. (2014). "Patterns of tree species composition across tropical African forests". In: *Journal of Biogeography* 41.12. Ed. by Peter Linder, pp. 2320–2331. DOI: 10.1111/jbi.12382.

Fick, S. E. and R. J. Hijmans (2017). "WorldClim 2: New 1-km spatial resolution climate surfaces for global land areas". In: *International Journal of Climatology* 37.12, pp. 4302–4315. DOI: http://dx.doi.org/10.1002/joc.5086.

Fuller, Douglas O. (1999). "Canopy phenology of some mopane and miombo woodlands in eastern Zambia". In: *Global Ecology and Biogeography* 8.3-4, pp. 199–209. DOI: 10.1046/j.1365-2699.1999.00130.x.

Gu, Lianhong et al. (2003). "Phenology of Vegetation Photosynthesis". In: *Phenology: An Integrative Environmental Science*. Springer Netherlands, pp. 467–485. DOI: 10.1007/978-94-007-0632-3_29.

Hillebrand, Helmut, Danuta M. Bennett, and Marc W. Cadotte (2008). "Consequences of dominance: A review of evenness effects on local and regional ecosystem processes". In: *Ecology* 89.6, pp. 1510–1520. DOI: 10.1890/07-1053.1.

Huffman, G. J. et al. (2015). *GPM IMERG Final Precipitation L3 1 day 0.1 degree x 0.1 degree V06 [Data set]*. Goddard Earth Sciences Data and Information Services Center (GES DISC). DOI: 10.5067/MODIS/MOD13Q1.006. (Visited on 10/30/2020).

Jeganathan, C., J. Dash, and P. M. Atkinson (2014). "Remotely sensed trends in the phenology of northern high latitude terrestrial vegetation, controlling for land cover change and vegetation type". In: *Remote Sensing of Environment* 143, pp. 154–170. DOI: 10.1016/j.rse.2013.11.020.

Kreft, Holger and Walter Jetz (2010). "A framework for delineating biogeographical regions based on species distributions". In: *Journal of Biogeography* 37.11, pp. 2029–2053. DOI: 10.1111/j.1365-2699.2010.02375.x.

Lüdecke, Daniel (2018). "ggeffects: Tidy Data Frames of Marginal Effects from Regression Models." In: *Journal of Open Source Software* 3.26, p. 772. DOI: 10.21105/joss.00772.

Morellato, Leonor Patrícia Cerdeira et al. (2016). "Linking plant phenology to conservation biology". In: *Biological Conservation* 195, pp. 60–72. DOI: 10.1016/j.biocon.2015.12.033.

Mukosha, J and A Siampale (2009). *Integrated land use assessment Zambia 2005–2008*. Lusaka, Zambia: Ministry of Tourism, Environment et al.

Murtagh, Fionn and Pierre Legendre (2014). "Ward's Hierarchical Agglomerative Clustering Method: Which Algorithms Implement Ward's Criterion?" In: *Journal of Classification* 31.3, pp. 274–295. DOI: 10.1007/s00357-014-9161-z.

Ogutu, Joseph O., Hans-Peter Piepho, and Holly T. Dublin (2013). "Responses of phenology, synchrony and fecundity of breeding by African ungulates to interannual variation in rainfall". In: *Wildlife Research* 40.8, p. 698. DOI: 10.1071/wr13117.

Parr, C. L. et al. (2014). "Tropical grassy biomes: misunderstood, neglected, and under threat". In: *Trends in Ecology and Evolution* 29, pp. 205–213. DOI: 10.1016/j.tree.2014.02.004Âă.

Pavlick, R. et al. (2013). "The Jena Diversity-Dynamic Global Vegetation Model (JeDi-DGVM): a diverse approach to representing terrestrial biogeography and biogeochemistry based on plant functional trade-offs". In: *Biogeosciences* 10.6, pp. 4137–4177. DOI: 10.5194/bg-10-4137-2013.

Pelletier, J. et al. (2018). "Carbon sink despite large deforestation in African tropical dry forests (miombo woodlands)". In: *Environmental Research Letters* 13, p. 094017. DOI: 10.1088/1748-9326/aadc9a.

Penuelas, J., T. Rutishauser, and I. Filella (2009). "Phenology Feedbacks on Climate Change". In: *Science* 324.5929, pp. 887–888. DOI: 10.1126/science.1173004.

R Core Team (2020). *R: A Language and Environment for Statistical Computing*. R Foundation for Statistical Computing. Vienna, Austria. URL: https://www.R-project.org/.

Rousseeuw, Peter J. (1987). "Silhouettes: A graphical aid to the interpretation and validation of cluster analysis". In: *Journal of Computational and Applied Mathematics* 20, pp. 53–65. DOI: 10.1016/0377-0427(87)90125-7.

Scheiter, Simon, Liam Langan, and Steven I. Higgins (2013). "Next-generation dynamic global vegetation models: learning from community ecology". In: *New Phytologist* 198.3, pp. 957–969. DOI: 10.1111/nph.12210.

Smith, B. and J. B. Wilson (1996). "A consumer's guide to evenness indices". In: *Oikos* 76, pp. 70–82. DOI: 10.2307/3545749.

White, Michael A. et al. (2009). "Intercomparison, interpretation, and assessment of spring phenology in North America estimated from remote sensing for 1982-2006". In: *Global Change Biology* 15.10, pp. 2335–2359. DOI: 10.1111/j.1365-2486.2009.01910.x.

Wilsey, Brian J. et al. (2005). "Relationships among indices suggest that richness is an incomplete surrogate for grassland biodiversity". In: *Ecology* 86.5, pp. 1178–1184. DOI: 10.1890/04-0394.

6 Supplementary Material

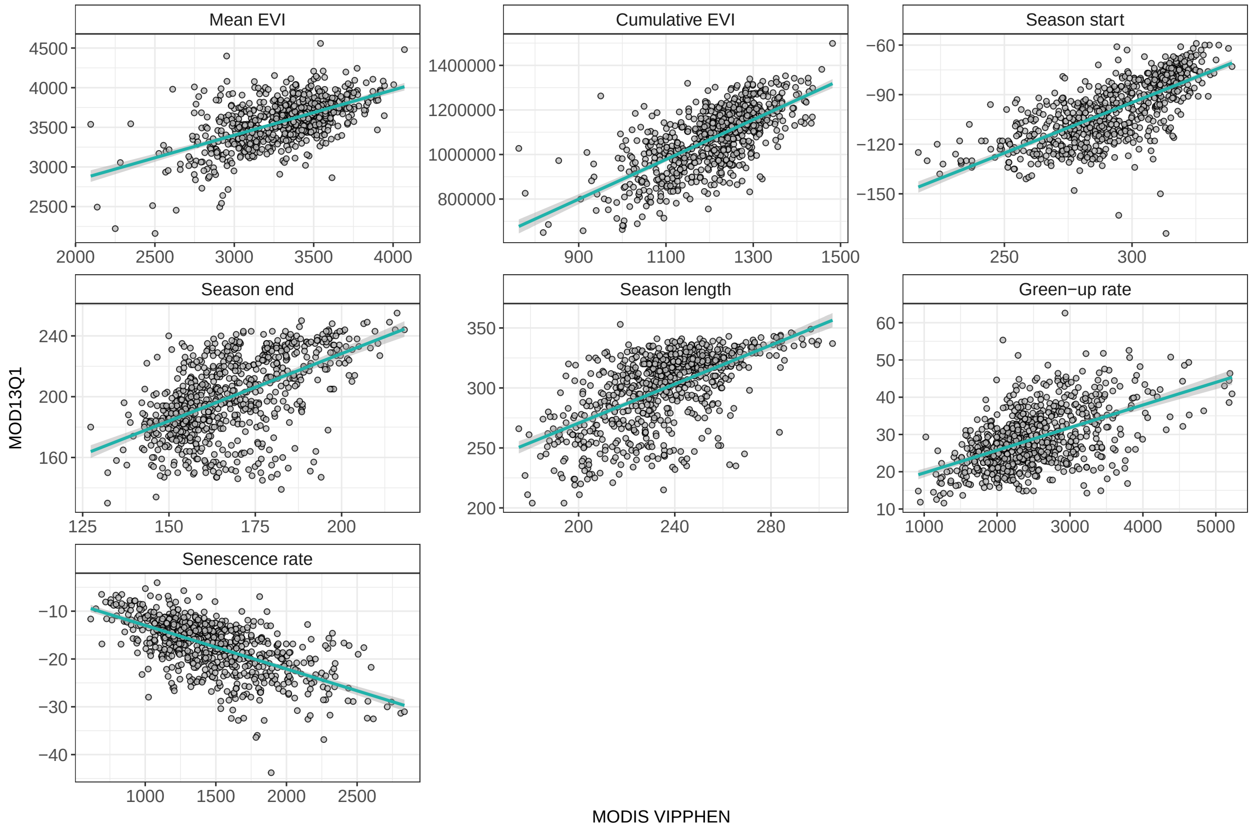

Figure S1: Scatter plots showing a comparison of phenological metrics from the MODIS VIPPHEN product (Didan and Barreto, 2016) and those extracted from the MOD13Q1 data (Didan, 2015), for each of the sites in our study. The cyan line shows a linear model of the data, with a 95% confidence interval.

Response	DoF	F	Prob.	R^2
Mean EVI	733	363.0	$p<0.05$	0.33
Cumulative EVI	733	639.0	$p<0.05$	0.47
Season start	733	772.7	$p<0.05$	0.51
Season end	733	322.8	$p<0.05$	0.31
Season length	733	393.0	$p<0.05$	0.35
Green-up rate	733	278.4	$p<0.05$	0.28
Senescence rate	733	459.5	$p<0.05$	0.39

Table S1: Model fit statistics for comparison of MODIS VIPPHEN and MOD13Q1 products across each of our study sites.

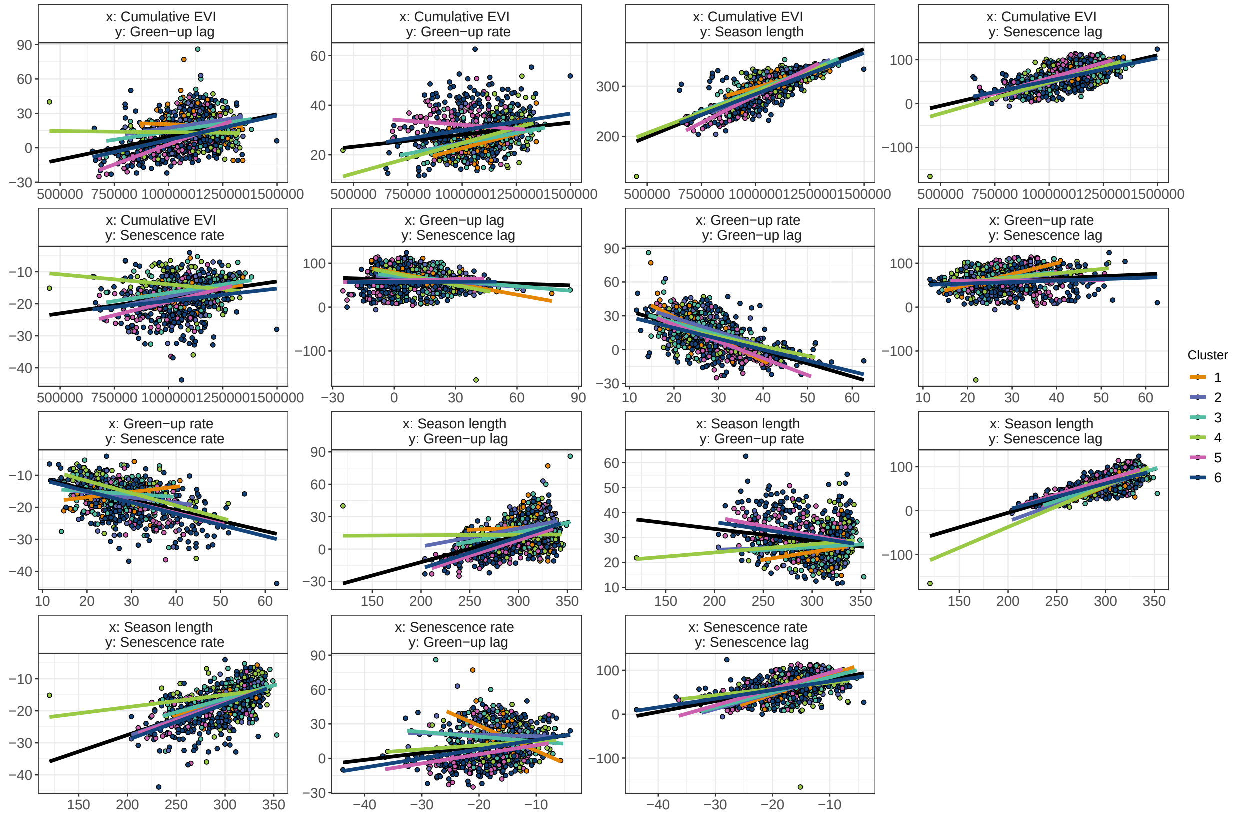

Figure S2: Scatter plots showing pairwise comparisons of the six phenological metrics used in this study, extracted from the MODIS MOD13Q1 product (Didan, 2015). Points represent study sites and are coloured by vegetation type. Linear regression line of best fit for all sites is shown as a black line, while linear regressions are shown for each vegetation type cluster as coloured lines.

Rank	Precipitation	Diurnal dT	Evenness	Richness	Richness:Cluster	logLik	AIC	ΔIC	W_i
1	✓		✓	✓	✓	**-9626**	**19274**	**0**	**0.521**
2	✓	✓	✓	✓	✓	-9625	19274	0	0.468
3	✓		✓		✓	-9631	19283	9	0.005
4	✓	✓	✓		✓	-9631	19283	10	0.004
5	✓		✓	✓		-9638	19288	14	0.000
6	✓	✓	✓	✓		-9638	19290	16	0.000
7	✓			✓		-9644	19298	24	0.000
8	✓	✓		✓		-9644	19299	25	0.000
9	✓					-9646	19301	27	0.000
10	✓		✓			-9646	19302	28	0.000

Table S2: Cumulative EVI model selection candidate models, with fit statistics. The overall best model is marked by bold text, while the best model with a richness:cluster interaction term is marked by underlined text

Rank	Precipitation	Diurnal dT	Evenness	Richness	Richness:Cluster	logLik	AIC	ΔIC	W_i
1	✓		✓	✓	✓	-3512	7046	0	0.510
2	✓	✓	✓	✓	✓	**-3511**	**7046**	**0**	**0.442**
3	✓		✓		✓	-3516	7052	6	0.025
4	✓	✓	✓		✓	-3515	7052	6	0.022
5	✓	✓	✓	✓		-3531	7077	31	0.000
6	✓		✓	✓		-3533	7079	33	0.000
7	✓	✓	✓			-3538	7088	43	0.000
8			✓	✓	✓	-3535	7089	44	0.000
9	✓	✓				-3540	7090	44	0.000
10	✓	✓		✓		-3539	7090	44	0.000

Table S3: Season length model selection candidate models, with fit statistics. The overall best model is marked by bold text, while the best model with a richness:cluster interaction term is marked by underlined text

Rank	Precipitation	Diurnal dT	Evenness	Richness	Richness:Cluster	logLik	AIC	ΔIC	W_i
1		✓	✓	✓	✓	-2509	5040	0	0.619
2	✓	✓	✓	✓	✓	**-2509**	**5042**	**2**	**0.228**
3		✓	✓		✓	-2512	5044	4	0.107
4	✓	✓	✓		✓	-2512	5045	5	0.042
5		✓	✓	✓		-2520	5051	11	0.002
6	✓	✓	✓	✓		-2520	5053	13	0.001
7		✓	✓			-2522	5055	15	0.000
8		✓				-2524	5055	15	0.000
9		✓		✓		-2523	5057	16	0.000
10	✓	✓	✓			-2522	5057	17	0.000

Table S4: Green-up rate model selection candidate models, with fit statistics. The overall best model is marked by bold text, while the best model with a richness:cluster interaction term is marked by underlined text

Rank	Precipitation	Diurnal dT	Evenness	Richness	Richness:Cluster	logLik	AIC	ΔIC	W_i
1	✓		✓	✓	✓	**-2293**	**4608**	**0**	**0.284**
2		✓	✓	✓	✓	-2293	4609	0	0.235
3			✓	✓	✓	-2294	4609	1	0.215
4	✓	✓	✓	✓	✓	-2293	4609	1	0.197
5			✓		✓	-2298	4614	5	0.021
6		✓	✓		✓	-2297	4614	5	0.020
7	✓		✓		✓	-2297	4614	6	0.014
8	✓	✓	✓		✓	-2297	4615	7	0.010
9	✓	✓	✓	✓		-2303	4619	11	0.001
10		✓	✓	✓		-2304	4619	11	0.001

Table S5: Senescence rate model selection candidate models, with fit statistics. The overall best model is marked by bold text, while the best model with a richness:cluster interaction term is marked by underlined text

Rank	Precipitation	Diurnal dT	Evenness	Richness	Richness:Cluster	logLik	AIC	ΔIC	W_i
1	✓	✓	✓	✓	✓	**-2951**	**5926**	**0**	**0.997**
2	✓	✓	✓	✓		-2962	5938	12	0.003
3	✓	✓	✓		✓	-2977	5977	50	0.000
4		✓	✓	✓	✓	-2979	5980	54	0.000
5	✓	✓	✓			-2989	5991	64	0.000
6		✓	✓	✓		-2990	5991	65	0.000
7	✓	✓				-3008	6027	100	0.000
8	✓	✓		✓		-3008	6027	101	0.000
9		✓	✓		✓	-3010	6041	114	0.000
10		✓	✓			-3021	6051	125	0.000

Table S6: Green-up lag model selection candidate models, with fit statistics. The overall best model is marked by bold text, while the best model with a richness:cluster interaction term is marked by underlined text

Rank	Precipitation	Diurnal dT	Evenness	Richness	Richness:Cluster	logLik	AIC	ΔIC	W_i
1		✓	✓		✓	**-3436**	**6892**	**0**	**0.464**
2		✓	✓	✓	✓	-3436	6894	2	0.188
3	✓	✓	✓		✓	-3436	6894	2	0.172
4	✓	✓	✓	✓	✓	-3436	6896	4	0.070
<u>5</u>		<u>✓</u>				<u>-3445</u>	<u>6897</u>	<u>5</u>	<u>0.040</u>
6		✓		✓		-3445	6899	7	0.016
7		✓	✓			-3445	6899	7	0.015
8	✓	✓				-3445	6899	7	0.015
9	✓	✓		✓		-3444	6901	9	0.006
10		✓	✓	✓		-3445	6901	9	0.006

Table S7: Senescence lag model selection candidate models, with fit statistics. The overall best model is marked by bold text, while the best model with a richness:cluster interaction term is marked by underlined text

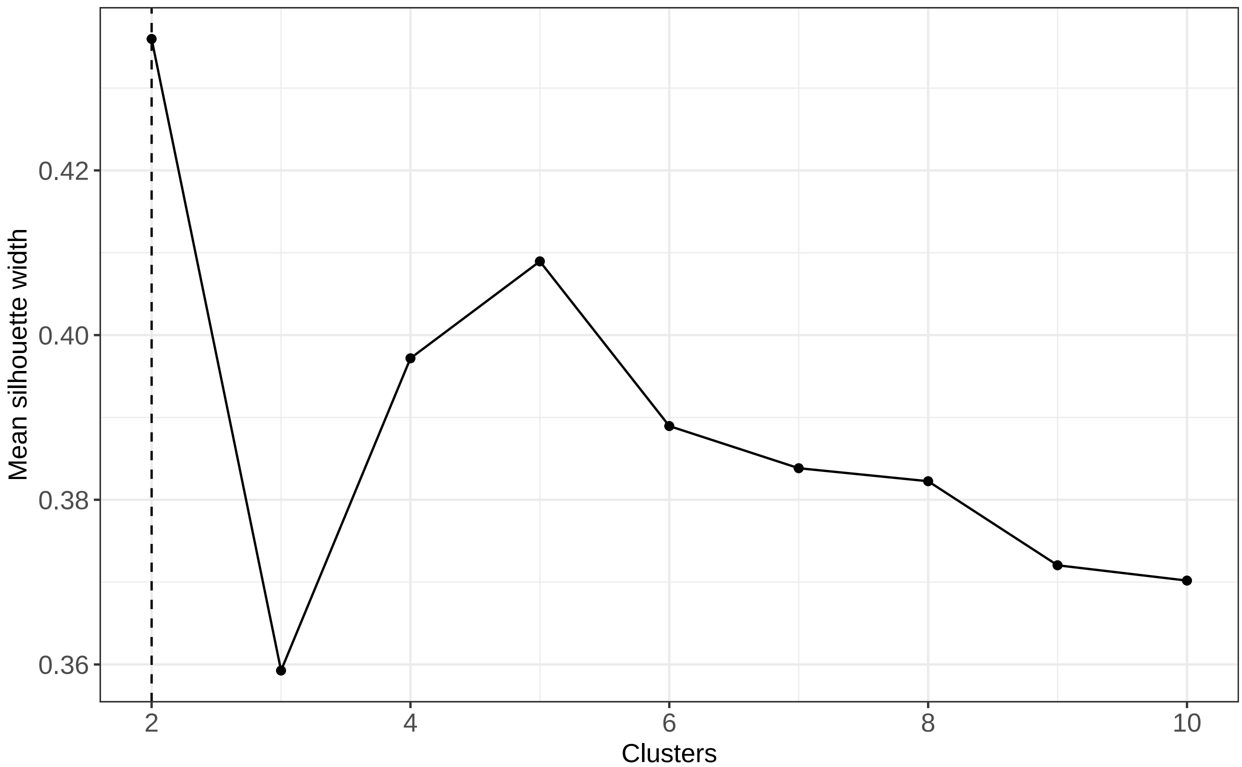

Figure S3: Mean silhouette width for agglomerative hierarchical clustering, specifying a varying number of clusters. The highest silhouette width, and therefore the number of clusters chosen in our analysis, is denoted by a dashed line.

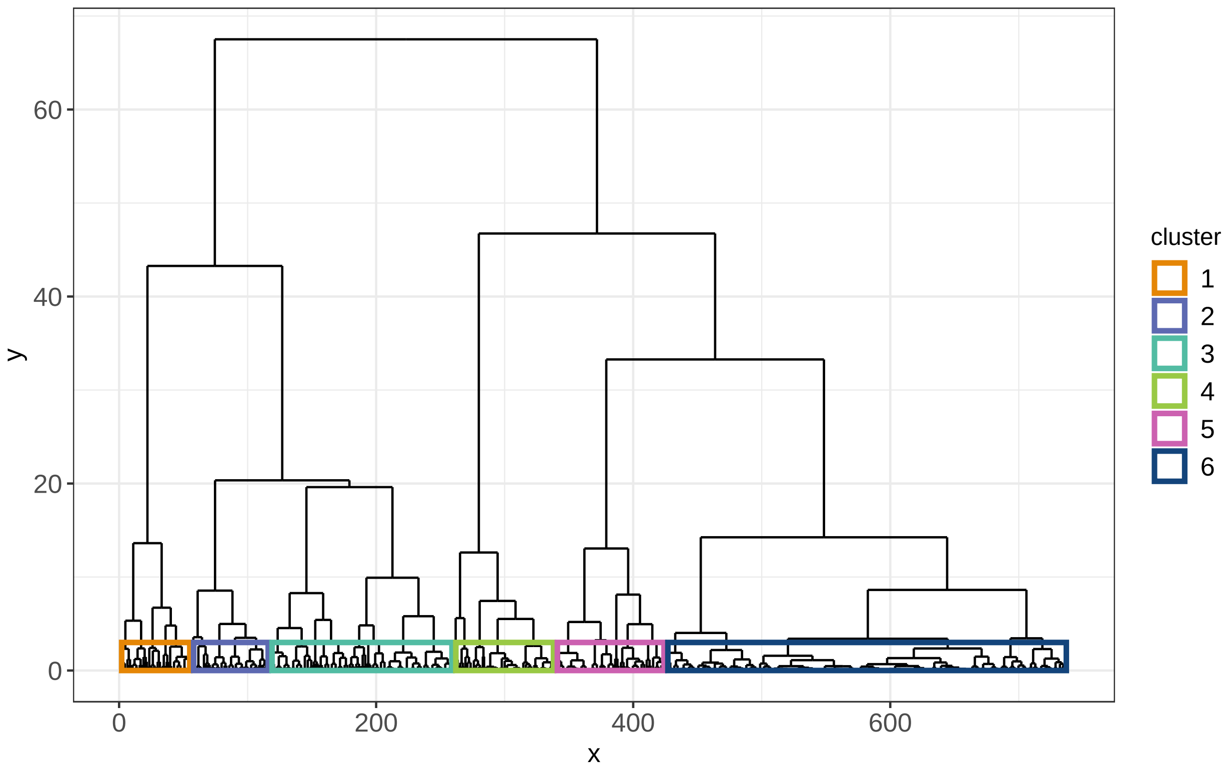

Figure S4: Dendrogram of hierarchical clustering of euclidean distances of NSCA (Non-Symmetric Correspondence Analysis) ordination axes, clustered using the Ward algorithm. Clusters are denoted by coloured boxes.

Response	Clusters	Estimate	SE	DoF	T ratio	Prob.
Cumulative EVI	1-2	1.1E-14	6.68E-14	697	0.17	0.98
	1-3	5.5E-14	6.33E-14	697	0.87	0.66
	2-3	4.4E-14	8.16E-14	697	0.54	0.85
Season length	1-2	-6.4E-18	1.56E-17	698	-0.41	0.91
	1-3	1.9E-17	1.48E-17	698	1.26	0.42
	2-3	2.5E-17	1.89E-17	698	1.32	0.38
Green-up rate	1-2	1.1E-18	4.89E-18	698	0.23	0.97
	1-3	-3.5E-18	4.59E-18	698	-0.76	0.73
	2-3	-4.6E-18	5.91E-18	698	-0.78	0.72
Senescence rate	1-2	3.7E-18	3.41E-18	698	1.09	0.52
	1-3	6.3E-18	3.21E-18	698	1.97	0.12
	2-3	2.6E-18	4.14E-18	698	0.63	0.80
Green-up lag	1-2	-7.3E-18	1.03E-17	698	-0.71	0.76
	1-3	6.0E-18	9.71E-18	698	0.62	0.81
	2-3	1.3E-17	1.25E-17	698	1.07	0.54
Senescence lag	1-2	2.9E-19	1.30E-17	698	0.02	1.00
	1-3	6.1E-18	1.23E-17	698	0.50	0.87
	2-3	5.9E-18	1.59E-17	698	0.37	0.93

Table S8: Comparisons of interaction marginal effects using post-hoc Tukey's tests.